Echo time spreading and the definition of transmission loss for broadband active sonar

Z. Y. Zhang

Defence Science and Technology Organisation

P.O. Box 1500, Edinburgh, SA 5111, Australia

ABSTRACT

In active sonar, the echo from a target is the convolution of the source waveform with the impulse responses of the target and the propagation channel. The transmitted source waveform is generally known and replica-correlation is used to increase the signal gain. This process is also called pulse compression because for broadband pulses the resulting correlation functions are impulse-like. The echo after replica-correlation may be regarded as equivalent to that received by transmitting the impulsive auto-correlation function of the source waveform. The echo energy is spread out in time due to different time-delays of the multipath propagation and from the scattering process from the target. Time spreading leads to a reduction in the peak power of the echo in comparison with that which would be obtained had all multipaths overlapped in time-delay. Therefore, in contrast to passive sonar where all energies from all significant multipaths are included, the concept of transmission losses in the active sonar equation needs to be handled with care when performing sonar performance modelling. We show modelled examples of echo time spreading for a baseline case from an international benchmarking workshop.

INTRODUCTION

The performance of an active sonar system is often illustrated by the power (or energy) budget afforded by a separable form of the sonar equation, such as the following,

$$SE = EL - [(NL - AG_N) \oplus RL] + MG - DT \quad (1)$$

where SE is the signal excess, EL is the sound pressure levels of the echo, $(NL - AG_N)$ is the in-beam noise level, i.e., noise level NL in the receiver bandwidth reduced by the receiver array gain AG_N against noise, RL is the in-beam reverberation level from scatterers on the source and receiver's beam pattern, $\oplus$ represents intensity summation. MG is the gain in signal to noise ratio (SNR) from matched filtering. The detection threshold, DT, is the SNR required at the *output* of the matched filter to achieve a certain probability of detection and false alarm for given signal and noise statistics.

The DT in Eq.(1) is defined at the *output* of the matched filter, which is the convention in Ainslie (2010), Lurton (2002), Bradley (1996), and the Radar literature (Barton 2005; DiFranco & Rubin 1968). When detection threshold is defined at the *input* to the temporal processor, as in Urick (1983), Burdic (1991), Waite (2002), and Etter (2003), the matched filtering gain is included in the detection threshold.

Traditionally, the echo level is often written as (Urick 1983; Burdic 1991; Waite 2002; Etter 2003),

$$EL = SL - TL_{S\to T} + TS - TL_{T\to R} \quad (2)$$

where SL is the source power level, $TL_{S\to T}$ is the one-way transmission loss from source to target, TS is the target strength, $TL_{T\to R}$ is the one-way transmission loss from target to receiver.

ECHO MODELLING ISSUES

In a sound channel, the transmitted pulse generally splits into multipath arrivals with different propagation angles and travel times that ensonify the target, which scatters and re-radiates each arrival to more multipath arrivals at the receiver. Hence the received echo is a multiple convolution of the transmitted source pulse with the following three impulse responses: (1) propagation from source to target; (2) target scattering; (3) propagation from target to receiver.

Whilst Eqs.(1) and (2) are instructive to help understand the power (or energy) budget of the sonar process, rigorous modelling of broadband coherent active sonar is more complex than computing the seemingly simple sonar equations because of the dependence of the sonar quantities on frequency, angle, and time.

In general, due to the presence of multipath with different propagation angles, the EL can not be computed from separable terms as in Eq.(2). Target scattering generally depends on incident and outward angles. Source beam patterns, propagation multipaths or multi-modes, and target scattering become coupled in angle domain and there is no separable equation to calculate EL from SL, TS, and TL. It is only when the target scattering cross section varies little across the angular domain of the significant multipaths, that the terms become separable (Ratilal et al 2002). In addition, effects of multiple scattering can be significant when the target is near an ocean boundary (Giddings & Shirron 2008; Hackman & Sammelmann 1988). Furthermore, in a multipath environment, the array signal gain also degrades from that computed for a single plane wave in free field (Zhang 2009).

Another complication arises from the dependence of the sonar quantities on frequency. The source level, propagation, target strength, noise and reverberation, array beam patterns and array gain, generally vary with frequency. Integration

with frequency is needed and the frequency dependence can only be ignored if the variation is small over the frequency band of interest.

The third complication comes from the time dependence or transient nature of pulse propagation, which is the focus of this paper.

Transmission Loss for Pulse Propagation

Traditional transmission loss, such as that for passive sonar, is defined for a harmonic wave of a single frequency, where all multipath contributions are added together because the signal is treated as of infinite time extent (Urick 1983; Jensen et al 2000). We may call these harmonic transmission losses. Coherent or phased additions, where the complex pressures are added, reveal constructive and destructive interferences between different paths. Incoherent addition, where the intensities are added, is often used to approximate the smoothing effects of averaging, e.g., over frequency, range, depth, (Harrison & Harrison 1995) or other statistical fluctuations. Incoherent addition can be over rays or modes where different types of phase information are discarded.

For pulses, one may define sound levels and transmission losses in terms of total energy integrated in time or frequency (Ainslie 2010; Marshall 1996). For simplicity we call these total transmission loss. One may also define transmission losses in terms of difference in energy spectral density (Badiey et al 1997), which correspond to harmonic transmission losses at the different component frequencies.

Peak pressures or intensity have also been used to represent sound levels (Madsen 2005) or to measure transmission losses (Hines et al 1997). We may call these peak transmission losses. For modelling the echo power level of an active sonar, after processing such as matched filtering, envelope detection, and averaging, what is relevant is the peak of the intensity sum of multipath arrivals within the sonar resolution cell.

The distinction between total and peak transmission loss is important for short pulses and can be illustrated by the simple example of propagation in an isovelocity waveguide. Whilst the total transmission loss may behave as cylindrical or "three halves law" spreading depending on the reflectivity of the bottom (Weston 1971;Brekhovskikh & Lysanov 2003;Harrison 2003), if the pulse is short enough so that all multipaths are separated, the peak transmission loss will be determined by the strongest direct path, leading to spherical spreading irrespective of bottom properties.

Two-way versus One-way Losses

It is often regarded as an indisputable fact in active sonar modelling that the two-way transmission loss is double the one-way loss. This is generally not true if losses are defined in terms of peak intensity.

The two-way impulse response pressure time series is a convolution in the time domain of the outward and return one-way impulse responses. For incoherent power summation, it can be shown that the intensity envelopes are also related by convolution (Harrison & Ainslie 2010). Generally the peak of a convolution is not a product of the peaks of the respective responses. Therefore peak transmission losses are not additive in dB.

For example, if the one-way response has a Gaussian envelope, the two-way response from convolution will also have a Gaussian envelope with its peak reduced by a factor of $\sqrt{2}$, i.e., the extra loss is a fixed value of 1.5 dB. If the one-way response is an exponential decay function, the peak of the two-way response is reduced by 4.3 dB relative to the one-way response (Weston 1965).

Convolution in time is equivalent to multiplication in the frequency domain. So if the pulses are narrowband, transmission losses defined for harmonic waves should be additive in dB.

To consider the relationship of one-way and two-way transmission losses defined in terms of total energy, it can be shown using the Fubini theorem (Kudryavtsev, LD 2001) that the integral of a convolution equals the product of the integrals of respective functions. Applying this property to the intensity impulse responses in time domain, e.g., Eq.(A3) of Harrison & Ainslie (2010), we conclude that transmission losses defined on total energy basis are additive in dB.

The same discussion and principle should apply to convolution with target responses, i.e., peak target strength generally is not additive in dB with transmission loss, but target strength defined for harmonic waves and total energy should be additive in dB.

Matched Filtering Gain and Correlation Loss

Under the following idealisations: (1) echoes from all multipath arrive at the same time; (2) each multipath suffers no distortion during its propagation, the echo would collapse into a single, time-delayed perfect replica of the transmitted pulse with its amplitude associated with total transmission loss. The matched filtering gain will be $10\log_{10}(BT)$, where B is the bandwidth and T is the duration of the transmitted pulse (Barger 1994; Waite 2002; Lurton 2002).

Multipath time spreading, time-varying, and dispersive properties of the channel introduce distortions to the pulse shape and consequently a correlation loss, CL (Ainslie 2010; Weston 1965)

$$MG = 10\log_{10}(BT) - CL \qquad (3)$$

It is more intuitive to understand correlation loss due to multipath time spreading in terms of the propagation of equivalent short pulses.

Equivalent Short Pulse

Matched filtering is equivalent to correlation with a scaled replica of the transmitted pulse. The output signal has a mainlobe whose effective duration is approximately the inverse of the signal bandwidth B and an amplitude that is proportional to the signal energy. The usual case is that the pulse length after correlation ($\approx 1/B$) is much shorter than the original pulse length (T), $1/B \ll T$. Hence the process is also called pulse compression. The scaling factor does not affect the output SNR because it affects the signal and noise in the same way.

From a modelling perspective, the scaling factor can be chosen such that after pulse compression, the signal energy is conserved and the noise power remain unchanged. The signal power (and the SNR) is increased by the pulse compression

ratio defined as the ratio of the pulse lengths before and after compression, i.e., approximately T/(1/B) = BT.

Because convolution and correlation processes are commutable, one may reverse the order of propagation with correlation and consider the propagation of an equivalent pulse whose shape resembles the autocorrelation function of the original pulse and whose amplitude increased by the square root of the pulse compression ratio relative to the original pulse to maintain the same total transmitted energy. The noise level remains unchanged because the original pulse and its autocorrelation function have the same bandwidth. The reverberation level is also unchanged because it is proportional to the transmitted pulse energy, that is, the reduced scattering area caused by the shorter duration balances the increased intensity.

Multipath Time Spreading

Each multipath in a sound channel ensonifies the target and arrives at the receiver at different times. If the transmitted pulse is sufficiently long such that all significant multipath arrivals overlap in time, the peak transmission loss will be essentially the same as the total transmission loss. Otherwise separation of significant multipath arrivals leads to a reduction in the intensity peak of the echo relative to that when all multipaths overlap. This reduction in echo intensity is called time spreading loss.

Time spreading loss can be estimated by the ratio of echo energy in the resolution cell over the total energy of the echo.

In summary, total transmission loss is the reduction in energy of the transmitted pulse due to geometric spreading, in-water absorption, and losses from boundaries, etc. Energy lost this way never reaches the receiver. Time spreading loss is the reduction in peak power from elongation of pulse due to multipath, target scattering, boundary interactions, and temporal fluctuations of the media. The time-stretched energy does reach the receiver, but the replica correlator is matched to the transmitted pulse, not the actual echo. The mismatch means that only a small portion of the available energy is processed in generating the peak of the correlation output.

Modelling Methods

Based on our discussion, the following methods can be used to model the peak echo level after correlation.

1. At the fundamental level, the echo can be modelled by simulating time series and passing them through the signal processing chain. The simulated echo is produced by convolution of impulse pressure responses or by Fourier synthesis of the product of frequency responses. This approach intrinsically accounts for transmission loss, time spreading losses, and processing gain. The temporal nature of pulse propagation is modelled and static concepts such as transmission loss and target strength do not come into play. This approach is accurate but also time consuming. In a way, this type of complexity is what an energy based approach such as the sonar equation is trying to avoid.

2. The time-varying echo intensity level is modelled by convolving the intensity envelope of the equivalent short pulse with the impulse intensity responses of the two-way multipaths and target scattering. The peak of the echo intensity is then chosen to compute the SNR. Because the equivalent short pulse is used, this approach also automatically accounts for transmission loss, time spreading loss, and processing gain.

3. The echo power level before correlation is computed from transmission losses and target strength based on total energy. The echo power level after correlation is then obtained by first adding the idealised processing gain for perfect replica and then corrected by the echo time spreading loss, which has to be estimated separately.

A word of caution is in order about the importance of using the equivalent short pulse in method 2. Often transmitted source pulses have durations of the order of seconds, which are greater than typical time spread induced by propagation and target scattering. Hence most significant multipath arrivals overlap. Even if one uses a sonar model that is based on picking the peak of the intensity convolution as in method 2, the length of the source pulse means that the echo obtained is still equivalent to the total transmission loss approach.

AN EXAMPLE ENVIRONMENT

To illustrate the concepts, we consider a simple model defined in the US Navy Office of Naval Research sponsored reverberation modelling workshop (ONR 2006; Perkins & Thorsos 2011) and subsequently used in scenarios for benchmarking sonar performance models (Zampolli et al 2010).

The water is 100 m deep with isovelocity of 1500 m/s, density of 1000 kg/m^3, and frequency dependent absorption modelled by Eq. (1.34) in Jensen et al (2000). The seabed is assumed to be a sandy bottom with sound speed of 1700 m/s, density of 2000 kg/m^3, and attenuation of 0.5 dB per wavelength.

Figure 1 shows the magnitude of the reflection coefficients at low grazing angles. The curve labelled “SB” (smooth bottom) represents the magnitude of the reflection coefficients from a sandy bottom with a smooth water-sediment interface, ignoring the effects of bottom roughness. The curve was computed from equations in standard texts (e.g., Brekhovskikh 1980). For reflections from a homogeneous half-space with a smooth water-bottom interface and bottom attenuation proportional to the first power of frequency, the reflection coefficient is independent of frequency.

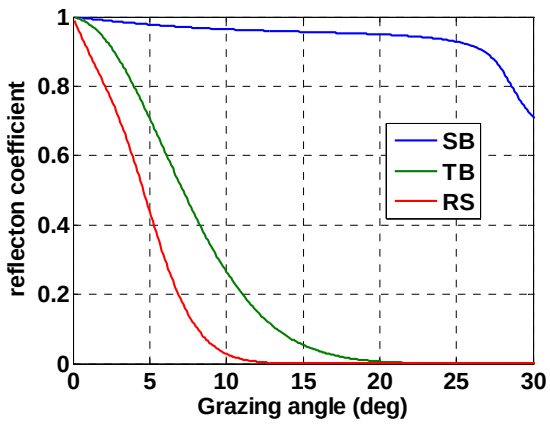

Figure 1. Magnitudes of the bottom and surface reflection coefficients at 3.5 kHz (SB – smooth bottom, TB – typical sandy bottom, RS - rough sea surface,).

The curve labelled "TB" is for a "typical sandy bottom" with a rough water-sediment interface described by one-dimensional power-law roughness spectra of rms height of 0.32 m and correlation length of 400 m (ONR 2006). Bubble effects were excluded. The curve labelled "RS" represents results for rough sea surfaces specified by Pierson-Moskowitz spectra for fully developed seas with a wind speed of 10 m/s at a height of 19.5 m. The reflection coefficients from the rough surfaces and bottoms were taken from the modelling workshop (ONR 2006). Both the "TB" and "RS" curves were generated using the second order small slope approximation at 3500 Hz.

ONE-WAY CHANNEL RESPONSE

Angular Spectra

To estimate the effective time spread of the channel, we first compute the envelope of the angular distribution of the eigenray intensity. For this purpose, we treat the grazing angle as a continuous variable and we call this envelope the angular spectra. We then translate the dependence on grazing angle into dependence on travel time.

At a particular range, there are four sets of multipaths that are characterised by their order of interactions with the boundaries, each path being represented by an integral. When the water depth is much greater than the acoustic wavelength, which is true in our case, each integral can be approximated by the contribution from an eigenray emanating from an image source introduced by the multiple boundary reflections (e.g., Brekhovskikh 1980).

The four sets of eigenrays differ by their source and receiver depth offsets in their slant range calculations. Each eigenray in sets 1 and 4 undergoes the same number of bottom and surface reflections. The eigenrays in set 2 have one extra bottom reflection and the eigenrays in set 3 have one extra surface reflection. As examples, we consider the eigenrays in sets 1 and 4. The essence of the physics of propagation in other eigenray sets is similar. Furthermore, we consider the special but representative case of both source and receiver at mid-water depths. In such cases, the direct path has a grazing angle of zero and the travel paths of the eigenrays consist of integer number of cycles.

At a range r, the path length of an eigenray with grazing angle θ is $r/\cos\theta$ and its intensity $S(\theta)$ can be written as,

$$S(\theta,r) = A\left(\frac{\cos^2\theta}{r^2}\right)\left[\exp\left(\frac{-2\alpha r}{\cos\theta}\right)\right]\left|V_b(\theta)V_s(\theta)\right|^{(2r/r_c)} \qquad (4)$$

Where A is a proportional constant, and the term in the first brackets is due to spherical spreading. The term in the second brackets is due to in-water absorption, α being the in-water absorption coefficient in neper/m. The remaining term is due to multiple bottom and surface reflections, where $V_b(\theta), V_s(\theta)$ are the bottom and surface amplitude reflection coefficients respectively. The number of and the ray cycle distance $r_c = 2H/\tan\theta$, H being the water depth, as illustrated in Figure 2.

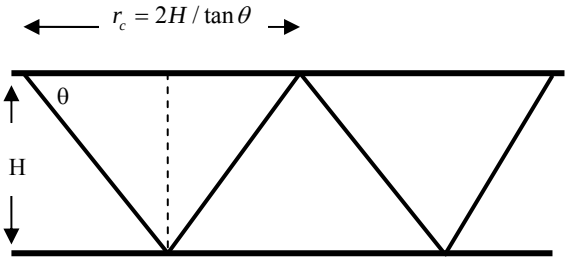

Figure 2. Illustration of cycle distance for a ray with grazing angle θ in a waveguide with water depth H.

We define the normalized angular spectra $S_n(\theta)$ as the angular distribution of the propagating energy normalized by the intensity of the direct ray,

$$S_n(\theta) = \frac{S(\theta,r)}{S(0,r)} = f_s(\theta)\, f_a(\theta)\, f_r(\theta) \qquad (5)$$

Where $f_s(\theta)$ is the contribution from geometric spreading,

$$f_s(\theta) = \cos^2\theta \qquad (6)$$

$f_a(\theta)$ is the contribution from in-water absorption,

$$f_a(\theta) = \exp(-2\alpha\,\Delta L) \qquad (7)$$

ΔL being the extra path length of a ray with grazing angle θ in comparison to that of the direct ray,

$$\Delta L = r(1/\cos\theta - 1) \qquad (8)$$

And $f_r(\theta)$ is the contribution from boundary reflections,

$$f_r(\theta) = \left|V_b(\theta)V_s(\theta)\right|^{(r\tan\theta/H)} \qquad (9)$$

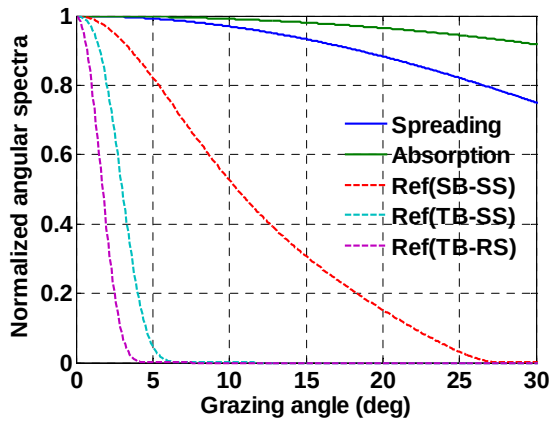

Figure 3. Comparison of the components of the normalized angular spectra for a frequency of 3.5 kHz and at a range of 10 km due to different propagation mechanisms: geometric spreading, in-water absorption, and reflections from different combinations of boundaries (smooth bottom with smooth surface, typical rough sandy bottom with smooth surface, typical rough sandy bottom with rough surface).

Figure 3 compares the components of the normalized angular spectra at a range of 10 km due to different propagation mechanisms. The line labelled "spreading" is from Eq.(6) and

the line labelled "absorption" is from Eq.(7). They represent the extra reduction in intensity from geometric spreading and in-water absorption due to the longer travel path for a ray with grazing angle θ in comparison to that of the direct ray. The dashed lines, from Eq.(9), represent effects of accumulated reflection losses from different combination of boundaries (smooth bottom with smooth surface, typical rough sandy bottom with smooth surface, typical rough sandy bottom with rough surface).

One can see from Fig.1 and Fig.2 that (1) boundary losses increase steeply with grazing angle and (2) the number of boundary reflections increases with grazing angle. The combined effect is that energy propagating at higher grazing angles is quickly stripped away. We also see that the effects of boundary losses dominate those of geometric spreading and in-water absorption.

Effective Angles

Figure 4 and 5 show the total angular spectra, i.e., Eq.(5), at various ranges without and with roughness-induced boundaries losses. Because energy propagating at steeper grazing angles is continuously being stripped away by boundary reflections, we see that (1) as range increases, the beam of energy propagating around horizontal becomes narrower; and (2) greater boundary losses leads to narrower beams at the same range.

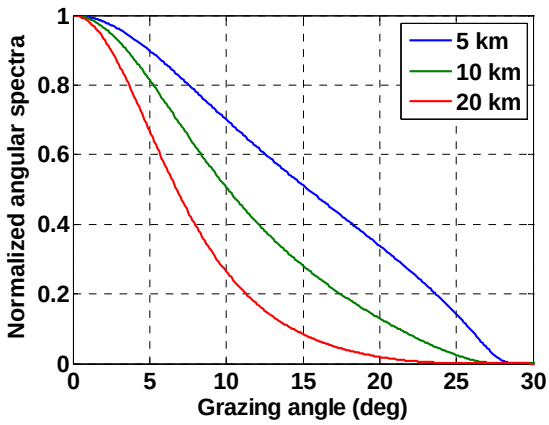

Figure 4. Normalized angular spectra at different ranges at 3.5 kHz for a smooth seafloor with a smooth sea surface.

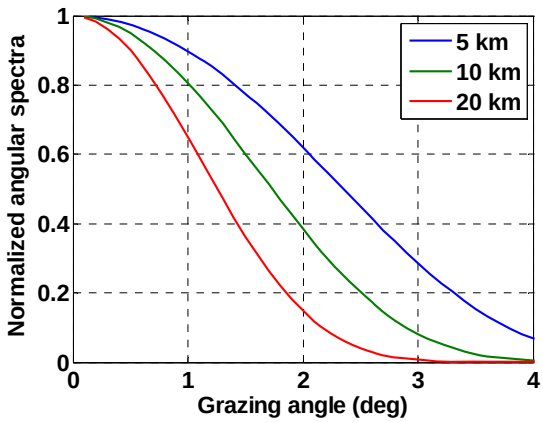

Figure 5. Normalized angular spectra at different ranges at 3.5 kHz for a typically rough sandy bottom with a wind-induced rough sea surface.

Effective Time Spread

Next we translate the dependence on grazing angle into dependence on multipath arrival time.

The extra time delay τ for a ray with grazing angle θ relative to the direct ray, is simply, from Eq.(8),

$$\tau = (r/c)(1/\cos\theta - 1) \tag{10}$$

We use Eq.(10) to convert the angular spectra in Fig.4 and 5 into dependence on time delay and the results are shown in Fig.6 and 7.

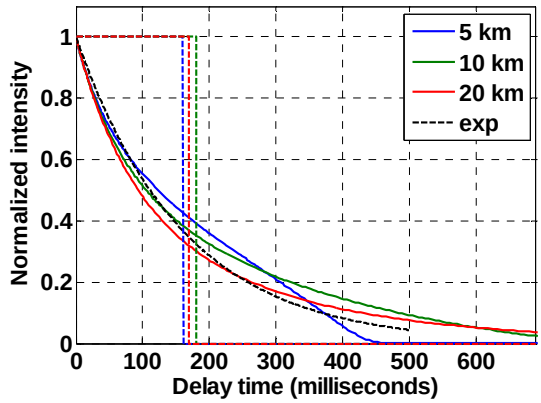

Figure 6. Envelope of multipath arrivals from one-way propagation at different ranges for a smooth seafloor with a smooth sea surface. The colored dashed lines represent the duration of unit rectangular pulses that have the same energy. The black dashed line is an exponential approximation with a decay constant of 160 ms.

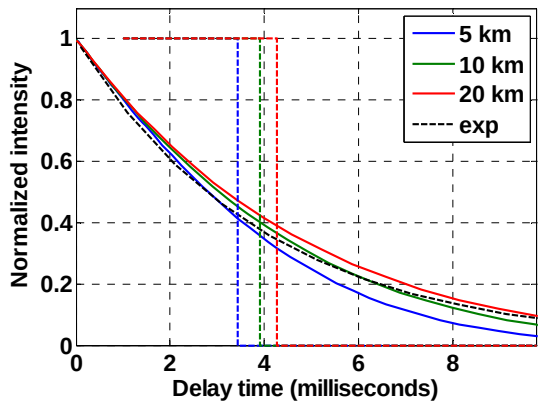

Figure 7. Same as Fig.6 but for a typically rough sandy bottom with a wind-induced rough surface. The black dashed line is an exponential approximation with a decay constant of 4 ms.

The color dashed lines in Figure 6 and 7 show the lengths of rectangular pulses that have the same energy as the decaying pulses shown by the solid lines of the same color. We may use these lengths as estimates of "effective time spread" induced by one-way propagation. We can see that for the cases considered, the effective time spreads correspond to the time intervals when the intensities of the decaying pulses drop to about 0.4 (4 dB down) of their peak value.

The black dashed lines in Fig. 6 and 7 are simple exponential fits to the colored lines based on visual inspection,

$$I(\tau) = \exp(-\tau / \tau_0) \tag{11}$$

where the time decay constants τ_0 are shown in the captions of Figs.6 to 7. We can see that the decay constants are close to the effective time spreads.

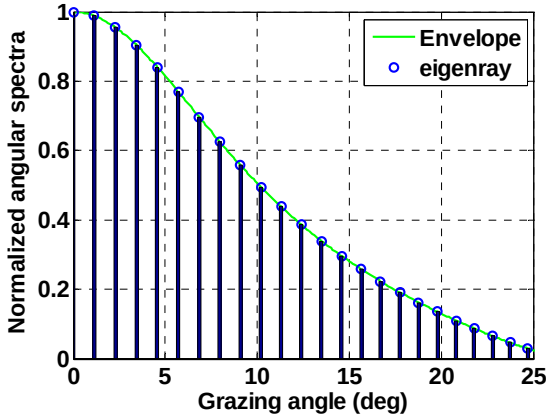

Figure 8. Normalized angular spectra and eigenray grazing angles at 10 km for a smooth seafloor with a smooth sea surface.

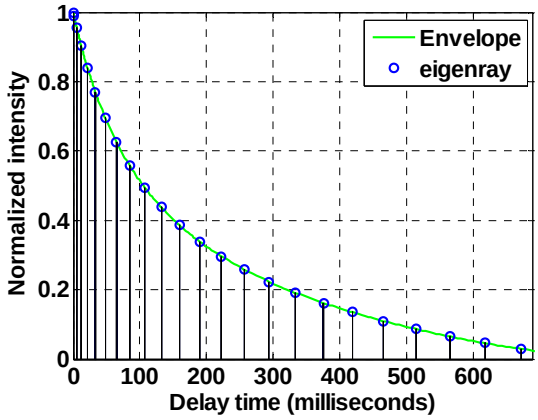

Figure 9. Envelope and multipath arrivals from one-way propagation at 10 km for a smooth seafloor with a smooth sea surface.

Figure 8 shows the normalized angular spectra and the eigenray grazing angles at 10 km for a smooth seafloor with a smooth sea surface. The eigenray angles were computed from

$$\theta_m = \arctan(2mH / r) \tag{12}$$

Figure 9 shows the envelope and eigenray arrivals in time domain by converting the results in Fig.8 using Eq.(10).

MODELLING ECHO TIME SPREADING LOSS

Analytical Bounds of Two-Way Response

We provide two analytical approximations to the two-way intensity impulse response, which serve as upper and lower bounds to the echo peak in assessing the echo time spreading loss.

The upper bound to the echo peak is provided by assuming the eigenrays are continuously distributed in grazing angle, which leads to a one-way intensity impulse response with an infinite peak (but still integrable with finite energy) and an exponential two-way intensity impulse response (Smith 1971; Weston 1989; Harrison & Nielsen 2007). The infinite peak is an artefact of regarding eigenrays as a continuum. In any case, the initial maximum response is finite and is that of the direct ray. From Figs. 8 and 9, we can see that the reason for the infinite peak is that eigenrays get denser in time at lower grazing angles. The exponential two-way impulse response has been used in predictions of SNR for test cases in benchmarking sonar performance (Zhang & Miyamoto, 2010).

The lower bound is provided by assuming that the eigenrays are uniformly distributed in time and using the exponential decay with the one-way effective time spreads obtained earlier as the one-way intensity impulse response. This will over-estimate the time spread because the method gives more weighting to the late-arriving eigenrays. The exponential one-way response leads to, upon convolution, a Rayleigh distributed two-way response.

Fig.10 and 11 show the evolution of the intensity envelopes of the pulses for smooth and rough boundaries, respectively. As we are interested in the echo time spreading losses relative to total echo energy, all the pulses have been normalized to have unit energy.

The darker blue line (barely visible in Fig.10 because of its short time duration) is a rectangular approximation to the compressed pulse for a waveform with bandwidth of 200 Hz. It has a time duration of 5 ms and an intensity level of L_0 = 23 dB re μPa^2-s so that its energy is unity. The green and cyan curves are exponential and Rayleigh functions which represent the analytical upper and lower bounds of the two-way impulse response. The red and magenta curves are obtained by convolving the initial rectangular pulse with the impulse responses and represent the upper and lower bounds of the resulting echo.

Time spreading loss can also be estimated from the ratio of the energy in the system resolution cell that contains the peak of the echo to the total energy of the echo. Hence as a crude approximation, we may predict the echo peak level using the following formula,

$$L_p = L_0 - 10\log_{10}[(\tau_R + 2\tau_0)/\tau_R] \tag{13}$$

Where L_0 = 23 dB re μPa^2-s is the intensity level of the rectangular pulse and $\tau_R = 5$ ms is its time resolution, τ_0 is the effective one-way time spread estimated in Fig. 6 and 7, $2\tau_0$ is an approximation to the two-way time spread. It is easy to confirm that the echo peak levels predicted by Eq.(13) match closely those in Fig. 10 and 11 based on Rayleigh impulse response functions.

The red curve can also be interpreted as the one-way pulse when the channel one-way impulse response is exponential. Comparison of its peak with the peak of the magenta curve in Fig.11 shows that when the time spreading losses are small, the two-way time spreading loss is approximately twice the one-way loss in dB. A similar comparison in Fig.10 shows that this is definitely not the case when the time spreading losses are large.

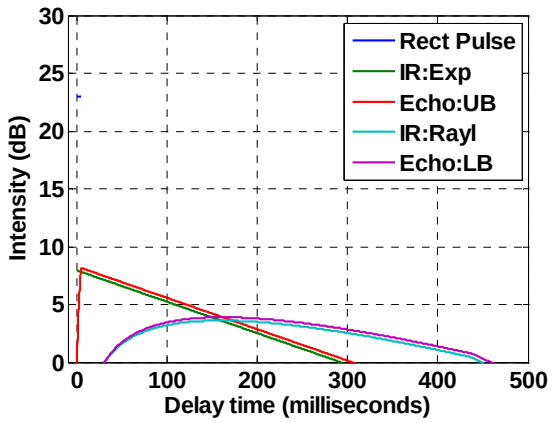

Fig.10. Evolution of pulse envelopes for smooth boundaries. The darker blue line (barely visible at 23 dB and zero time delay) is a rectangular pulse of 5 ms duration. The green and cyan curves are exponential and Rayleigh two-way impulse responses. The red and magenta curves are upper and lower bounds of the echo envelope.

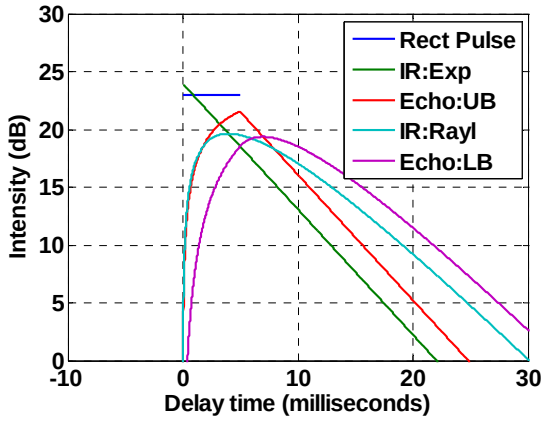

Fig.11. Similar to Figure 10, with reflection losses from rough bottom and surface boundaries included.

LIMITATIONS AND DISCUSSIONS

Time Spreading Due to Other Factors

In addition to multipath propagation, other factors also stretch and distort the echoes, for example, reflections from moving sea surfaces with air bubbles (Culver & Bradley 2005); reflections from sea bottoms with rough interfaces, multi-layering and inhomogeneities (Vidmar & Knobles 1989; McCammon 1990); temporal and spatial fluctuations in the water (Flatte 1983; Flatte et al 1987); and scattering from targets of complex structures with distributed scattering centres of various scattering processes and mechanisms (Urick 1983: Fig.2.6; Hodges 2010: Fig.13.27).

Post-detection Integration

Sometimes post-detection integration is used to collect the echo energy split by the multi-paths to reduce the time spreading loss (Barger 1997). Post-detection integration requires accurate prediction of the extent of time spread so that an optimum integration time can be chosen. The optimum integration length depends on the environment, the target, and the pulse waveform. If the integration time is too long, extra noise is introduced and the signal-to-noise ratio is reduced. If the integration time is too short, the noise is reduced but so is the signal energy. Post-detection integration is an incoherent process, when applied appropriately, introduces a gain of the form $5\log_{10}(BT)$ (Weston 1965;Waite 2002). The net effect is to essentially halve the time spreading loss (Weston 1965) in terms of detectability.

Model-Based Matched Filtering

Another technique to reduce time spreading loss is model-based matched filtering where a predicted echo rather than the transmitted pulse is used as the replica to capture the split energy coherently (Hermand & Roderick 1993; Baggenstoss 1994). Model-based matched filtering requires accurate prediction of echo shape and involves correlation of the received echo with a modelled replica from the convolution of the transmitted pulse with the impulse response of the channel. To predict the echo shape, one would need high-fidelity modelling and sufficient information about the environment and the target.

CONCLUDING REMARKS

Angular and time spreading of multipath and the transient nature of pulse propagation complicates modelling of sonar echoes, even without considering the time-dispersive and angle-dependent nature of scattering from realistic targets.

Modelling the performance of high-resolution pulses dictates thinking in terms of convolution of impulse responses and the concept of transmission losses needs to be handled with care. In particular, multipath time spreading leads to loss of peak echo power when significant multipath arrivals lie outside the peak resolution cell.

Commutation of convolution and correlation means that one effective strategy is to model the transmission of a suitably scaled compressed pulse. We analysed the angular and time spread of multipaths for a baseline environment from an ONR workshop. Using analytical upper and lower bounds to the envelope of the impulse response, we estimated the echo time spreading loss for a typical pulse resolution.

We conclude with a comment on the effects of multipath time spreading on the modelling of diffuse reverberation. Because the scatterers causing reverberation are generally extended in size, reverberation is continuous in time and energy spread out of one cell is still captured by the neighbouring time cells. Hence we expect total transmission loss can be used to model reverberation without loss of much accuracy, which should expedite the modelling of reverberation.

REFERENCES

Ainslie, MA 2010, *Principles of Sonar Performance Modeling*, Springer-Praxis.

APL-UW 1994, *High-Frequency Ocean Environmental Acoustic Models Handbook*, Applied Physics Laboratory, University of Washington, Seattle, Technical Report APL-UW TR 9407.

Baggenstoss, PM 1994, "On detecting linear frequency modulated waveforms in frequency and time dispersive channels: Alternatives to segmented replica correlation," *IEEE Journal of Oceanic Engineering*, vol. 19, pp. 591–598.

Badiey, M, Bongiovanni, KP, and Siegmann, WL 1997, "Analysis and model/data comparison of broadband acoustic propagation at the Atlantic Generating Station (AGS) site," *J. Acoust. Soc. Am.* **101,** 1921-1935.

Barger, JE 1997, "Sonar Systems", in *Encyclopedia of acoustics*, ed. Malcolm J. Crocker, (John Wiley, New York). pp. 559-579.

Barton, DK 2005, *Radar System Analysis and Modelling* (Artech House, Norwood, MA).

Bradley, M 1996, "*Environmental Acoustics Pocket Handbook,*" Planning Systems Incorporated, 2nd edition

Brekhovskikh, LM 1980, *Waves in Layered Media*, 2nd ed. (Academic, New York)

Brekhovskikh, LM and Lysanov, YP 2003, *Fundamentals of Ocean Acoustics*, 3rd ed. (Springer-Verlag, Berlin)

Burdic, WS 1991, *Underwater Acoustic System Analysis* (Prentice-Hall, NJ), 2nd Ed.

DiFranco, JV and Rubin, WL 1968, *Radar Detection*, Prentice-Hall.

Cox, H 1989, "Fundamentals of bistatic active sonar",in *Underwater Acoustic Data Processing,* Proceedings of NATO Advanced Science Institute Series E: Applied Sciences, Vol.161, ed. Y.T. Chan, Kluwer Academic Publishers, Dordrecht, The Netherlands, pp.3-24.

Culver, RL and Bradley, DL 2005, "On the relationship between signal bandwidth and frequency correlation for ocean surface forward scattered signals", *J. Acoust. Soc. Am.* 118, 129-138.

Etter, PC 2003, *Underwater Acoustic Modelling and Simulation*, 3rd edition, Spon Press.

Flatte, SM 1983, "Wave propagation through random media: Contributions from ocean acoustics," *Proceedings of the IEEE* , 71, 1267-1294.

Flatte, S, Reynolds, S, Dashen, R, Buehler, B, and Maciejewski, P 1987, "AFAR measurements of intensity and intensity moments," *J. Acoust. Soc. Am.* 82, 973–980.

Giddings, TE and Shirron, JJ 2008, "A model for sonar interrogation of complex bottom and surface targets in shallow-water waveguides", *J. Acoust. Soc. Am.* 123, pp. 2024-2034.

Hackman, RH and Sammelmann, GS 1988, "Multiple scattering analysis for a target in an oceanic waveguide," *J. Acoust. Soc. Am.* 84, pp. 1813-1825.

Harrison, CH and Harrison, JA 1995, "A simple relationship between frequency and range averages for broadband sonar," *J. Acoust. Soc. Am.* **97**:1314-1317.

Harrison, CH 2003**,** "Closed-form expressions for ocean reverberation and signal excess with mode-stripping and Lambert's law," *J. Acoust. Soc. Am.* **114**, 2744-2756.

Harrison, C. H., and Nielsen, P. L. (2007). "Multipath pulse shapes in shallow water: Theory and simulation," *J. Acoust. Soc. Am.* 121, 1362–1373.

Harrison, CH and Ainslie, MA 2010, "Fixed time versus fixed range reverberation calculation: Analytical solution", *J. Acoust. Soc. Am.* 128, 28.

Hermand, JP and Roderick, WI 1993, "Acoustic model-based matched filter processing for fading time-dispersive ocean channels.", *IEEE J. Oceanic Eng.*, 18(4), 447–465.

Hines, PC, Collier, AJ, and Theriault, JA 1997, "two-way time spreading and path loss in shallow water at 20-40 khz", *IEEE J. Oceanic Eng.* **22**, 299-308.

Hodges, RP 2010, *Underwater Acoustics: Analysis, Design and Performance of Sonar*, Wiley, Hoboken, NJ.

Jensen, F, Kuperman, W, Porter, M, and Schmidt, H 2000, *Computational Ocean Acoustics*, Springer-Verlag.

Kudryavtsev, LD 2001, "Fubini theorem", in Hazewinkel, Michiel, *Encyclopaedia of Mathematics*, Springer.

Lurton, X 2002, *An Introduction to Underwater Acoustics: Principles and Applications*, Springer.

Madsen, PT 2005, "Marine mammals and noise: Problems with root mean square sound pressure levels for transients", *J. Acoust. Soc. Am.* 117, 3952.

Marshall, WJ 1996, "Descriptors of impulsive signal levels commonly used in underwater acoustics," *IEEE Journal of Oceanic Engineering*, **21**, 108 –110.

McCammon, DF 1990, "A sediment time-angle spreading model", *J. Acoust. Soc. Am.* 87, 1126-1133.

ONR 2006, US Navy Office of Naval Research, Reverberation modelling workshop, environment definition: ftp://ftp.ccs.nrl.navy.mil/pub/ram/RevModWkshp_I/Problem_Definition_Documents

Perkins, JS and Thorsos EI 2011, 'Reverberation modeling workshops (A)', *J. Acoust. Soc. Am.* 129, pp. 2363-2363.

Ratilal, P., Lai, Y., and Makris, N.C. (2002), "Validity of the sonar equation and Babinet's principle for scattering in a stratified medium", *J. Acoust. Soc. Am.* 112, 1797.

Smith, PW 1971, "The averaged impulse response of a shallow-water channel", *J. Acoust. Soc. Am.* 50, 332-336.

Urick, RJ 1983, *Principles of Underwater Sound*, 3rd edition, McGraw-Hill.

Vidmar, PJ and Knobles, DP 1989, "Analysis of the time spread of bottom interacting signals from an abyssal plain environment", *J. Acoust. Soc. Am.* 86, 295-305.

Weston, DE 1965, "Correlation Loss in Echo Ranging," *J. Acoust. Soc. Am.* 37, 119-124.

Weston, DE 1971, "Intensity-range relations in oceanographic acoustics," *J. Sound Vib.* **18**, 271–287.

Weston, DE 1989, "Acoustic coherence loss due to ocean boundary interactions", in *Underwater Acoustic Data Processing,* Proceedings of NATO Advanced Science Institute Series E: Applied Sciences, edited by Y.T. Chan (Kluwer Academic, Dordrecht, The Netherlands), pp.55-68.

Waite, AD 2002, *SONAR for Practising Engineers*, John Wiley & Sons Inc, 3rd Edition.

Zampolli, M, Ainslie, MA and Schippers, P 2010, 'Scenarios for benchmarking range-dependent active sonar performance models', *Proc. Institute of Acoustics,* 32, Pt. 2, 2010.

Zhang, ZY 2009, "Estimating sonar system losses due to signal spatial decorrelation", *Proc. Australian Acoustical Society*, 23-25 November 2009, Adelaide, Australia.

Zhang, ZY and Miyamoto, R 2010, "Predictions of sonar performance for the baseline test case: the significance of echo time spreading losses", *Proc. Institute of Acoustics,* 32, Pt. 2, 2010.